Use of coherent control for selective two-photon fluorescence microscopy in live organisms

Jennifer P. Ogilvie

Laboratoire d'Optique et Biosciences, Centre National de la Recherche Scientifique Unité Mixte de Recherche 7645 – Institut National de la Santé et de la Recherche Médicale U696 – Ecole Polytechnique, 91128 Palaiseau Cedex, France
and
Department of Physics/Biophysics Research Division, University of Michigan, Ann Arbor, MI 48109
jogilvie@umich.edu

Delphine Débarre, Xavier Solinas, Jean-Louis Martin, Emmanuel Beaurepaire and Manuel Joffre

Laboratoire d'Optique et Biosciences, Centre National de la Recherche Scientifique Unité Mixte de Recherche 7645 – Institut National de la Santé et de la Recherche Médicale U696 – Ecole Polytechnique, 91128 Palaiseau Cedex, France
manuel.joffre@polytechnique.fr

Abstract: We demonstrate selective fluorescence excitation of specific molecular species in live organisms by using coherent control of two-photon excitation. We have acquired quasi-simultaneous images in live fluorescently-labeled *Drosophila* embryos by rapid switching between appropriate pulse shapes. Linear combinations of these images demonstrate that a high degree of fluorophore selectivity is attainable through phase-shaping. Broadband phase-shaped excitation opens up new possibilities for single-laser, multiplex, *in-vivo* fluorescence microscopy.

OCIS codes: (320.5540) Pulse shaping; (180.2520) Fluorescence microscopy; (190.4180) Multiphoton processes

References and links

1. K. A. Walowicz, I. Pastirk, V. V. Lozovoy, M. Dantus, "Multiphoton intrapulse interference. 1. Control of multiphoton processes in condensed phases," J. Phys. Chem. A **106**, 9369-9373 (2002).
2. V. V. Lozovoy, I. Pastirk, K. A. Walowicz, M. Dantus, "Multiphoton intrapulse interference. Ii. Control of two- and three-photon laser induced fluorescence with shaped pulses," J. Chem. Phys. **118**, 3187-3196 (2003).
3. J. Chen, H. Kawano, Y. Nabekawa, H. Mizuno, A. Miyawaki, T. Tanabe, F. Kannari, K. Midorikawa, "Selective excitation between two-photon and three-photon fluorescence with engineered cost functions," Opt. Express **12**, 3408-3414 (2004).
4. J. P. Ogilvie, K. Kubarych, A. Alexandrou, M. Joffre, "Fourier transform measurement of two-photon excitation spectra: Applications to microscopy and optimal control," Opt. Lett. **30**, 911-913 (2005).
5. A. Assion, T. Baumert, M. Bergt, T. Brixner, B. Kiefer, V. Seyfried, M. Strehle, G. Gerber, "Control of chemical reactions by feedback-optimized phase-shaped femtosecond laser pulses," Science **282**, 919-922 (1998).
6. N. Dudovich, D. Oron, Y. Silberberg, "Single-pulse coherently controlled nonlinear Raman spectroscopy and microscopy," Nature **418**, 512-514 (2002).
7. I. Pastirk, J. M. Dela Cruz, K. A. Walowicz, V. V. Lozovoy, M. Dantus, "Selective two-photon microscopy with shaped femtosecond pulses," Opt. Express **11**, 1695-1701 (2003).
8. J. M. Dela Cruz, I. Pastirk, V. V. Lozovoy, K. A. Walowicz, M. Dantus, "Multiphoton intrapulse interference 3: Probing microscopic chemical environments," J. Phys. Chem. A **108**, 53-58 (2004).
9. J. M. Dela Cruz, I. Pastirk, M. Comstock, V. V. Lozovoy, M. Dantus, "Use of coherent control methods through scattering biological tissue to achieve functional imaging," Proc. Natl. Acad. Sci. **101**, 16996-17001 (2004).
10. D. Meshulach, Y. Silberberg, "Coherent quantum control of two-photon transitions by a femtosecond laser pulse," Nature **396**, 239-242 (1998).

#9986 - $15.00 USD Received 20 December 2005; revised 13 January 2006; accepted 14 January 2006

11. R. S. Judson, H. Rabitz, "Teaching lasers to control molecules," Phys. Rev. Lett. **68**, 1500-1503 (1992).
12. M. Comstock, V. V. Lozovoy, I. Pastirk, M. Dantus, "Multiphoton intrapulse interference 6; binary phase shaping," Opt. Express **12**, 1061-1066 (2004).
13. M. A. Dugan, J. X. Tull, W. S. Warren, "High-resolution acousto-optic shaping of unamplified and amplified femtosecond laser pulses," J. Opt. Soc. Am. B **14**, 2348-2358 (1997).
14. E. Frumker, D. Oron, D. Mandelik, Y. Silberberg, "Femtosecond pulse-shape modulation at kilohertz rates," Opt. Lett. **29**, 890-892 (2004).
15. E. Frumker, E. Tal, Y. Silberberg, S. Majer, "Femtosecond pulse-shape modulation at nanosecond rates", Opt. Lett. **30**, 2796-2798 (2005).
16. F. Verluise, V. Laude, Z. Cheng, C. Spielmann, P. Tournois, "Amplitude and phase control of ultrashort pulses by use of an acousto-optic programmable dispersive filter: Pulse compression and shaping," Opt. Lett. **25**, 575-577 (2000).
17. D. P. Kiehart, C. G. Galbraith, K. A. Edwards, W. L. Rickoll, R. A. Montague, "Multiple forces contribute to cell sheet morphogenesis for dorsal closure in drosophila," J. Cell Biol. **149**, 471-490 (2000).
18. E. Wieschaus, C. Nusslein-Volhard, "Drosophila: A practical approach", Oxford, Oxford University Press (1998).
19. I. Davis, "Visualizing fluorescence in drosophila - optical detection in thick specimens". In Protein localization by fluorescence microscopy: A practical approach, Edited by Oxford University Press, 133-162 (2000).
20. W. Zipfel, R. M. Williams, R. Christie, A. Y. Nikitin, B. T. Hyman, W. W. Webb, "Live tissue intrinsic emission microscopy using multiphoton-excited native fluorescence and second harmonic generation," Proc. Natl. Acad. Sci. **100**, 7075-7080 (2003).
21. C. Xu, W. Zipfel, J. B. Shear, R. M. Williams, W. W. Webb, "Multiphoton fluorescence excitation: New spectral windows for biological nonlinear microscopy," Proc. Natl. Acad. Sci. **93**, 10763-10768 (1996).
22. E. Spiess, F. Bestvater, A. Heckel-Pompey, K. Toth, M. Hacker, G. Stobrawa, T. Feurer, C. Wotzlaw, U. Berchner-Pfannschmidt, T. Porwol, et al., "Two-photon excitation and emission spectra of the green fluorescent protein variants eCFP, eGFP and eYFP," J. of Microscopy **217**, 200-204 (2005).
23. P. Tournois: "Acousto-optic programmable dispersive filter for adaptive compensation of group delay time dispersion in laser systems," Opt. Comm. **140**, 245-249 (1997).
24. R. L. Fork, O. E. Martinez, J. P. Gordon, "Negative dispersion using pairs of prisms," Opt. Lett. **9**, 150 (1984).
25. A. C. Millard, D. N. Fittinghoff, J. A. Squier, M. Muller, A. L. Gaeta, "Using GaAsP photodiodes to characterize ultrashort pulses under high numerical aperture focusing in microscopy," J. of Microscopy **193**, 179-181 (1999).
26. W. Supatto, D. Débarre, B. Moulia, E. Brouzés, J.-L. Martin, E. Farge, E. Beaurepaire, "In vivo modulation of morphogenetic movements in drosophila embryos with femtosecond laser pulses," Proc. Natl. Acad. Sci. **102**, 1047-1052 (2005).
27. W. R. Zipfel, Williams, R. M., W. W. Webb, "Nonlinear magic: Multiphoton microscopy in the biosciences," Nat. Biotech. **21**, 1369-1377 (2003).
28. J. K. Ranka, R. S. Windeler, A. J. Stentz, "Visible continuum generation in air-silica microstructure optical fibers with anomalous dispersion at 800 nm," Opt. Lett. **25**, 25-27 (2000).
29. S. Huang, A. A. Heikal, W. W. Webb, "Two-photon fluorescence spectroscopy and microscopy of NAD(P)H and flavoprotein," Biophys. J. **82**, 2811-2825 (2002).

The growing field of coherent control has demonstrated precise manipulation of nonlinear excitation through pulse-shaping methods. These methods tailor the spectral phase and/or amplitude of laser pulses to optimize a particular pathway while suppressing undesirable outcomes. Among the successes of this field have been the control of multiphoton excited fluorescence [1-4], and the branching ratios of chemical reactions [5]. Coherent control methods have recently found applications in nonlinear microscopy, where shaping of the spectral phase has been used to enhance image contrast in coherent anti-Stokes Raman scattering microscopy [6]. Selective multiphoton microscopy has also been demonstrated through the selective excitation of different fluorescent probes [7], as well as through the pH-dependent excitation of a dye, thus probing its local chemical environment [7,8]. Although imaging of biological organisms using this approach has not previously been reported, it has been shown that spectrally tailored pulses maintain their spectral phase-shaping after propagation through scattering media [9], allaying fears that they cannot be used for imaging within complex samples.

#9986 - $15.00 USD Received 20 December 2005; revised 13 January 2006; accepted 14 January 2006

In this work we show that spectral phase-shaping of broadband laser pulses can be used to selectively excite the two-photon fluorescence of distinct chromophores in live *Drosophila* embryos labeled with enhanced green fluorescent protein (eGFP). This is achieved using a laser-scanning microscope and an acousto-optic pulse shaper allowing fast switching between two appropriate pulse shapes. We thus demonstrate the quasi-simultaneous acquisition of two images of the embryo under excitation conditions enhancing respectively the eGFP fluorescence and the endogenous fluorescence.

Coherent control of 2-Photon Excited Fluorescence (2PEF) can be easily understood in terms of the Second Harmonic (SH) spectrum of the exciting field [1,4,10]. Let us call $E(t)$ the electric field associated with the shaped pulse, and $E^{(2)}(t)=E(t)^2$ the SH field. In the frequency domain, these fields read respectively $E(\omega)=|E(\omega)|exp[i\varphi(\omega)]$ and $E^{(2)}(\omega)$, where $\varphi(\omega)$ is the spectral phase. The SH spectrum is given by

$$\left|E^{(2)}(\omega)\right|^2 \propto \left|\int_{-\infty}^{\infty}\left|E(\omega')\right|\left|E(\omega-\omega')\right|\exp\left[i\{\varphi(\omega')+\varphi(\omega-\omega')\}\right]d\omega'\right|^2 \qquad (1)$$

When there is no resonant intermediate level – a typical case in MPM - the chromophore is effectively driven by the SH field, so that 2PEF is simply proportional to the overlap integral between $|E^{(2)}(\omega)|^2$ and the two-photon excitation spectrum of the chromophore [1,4]. Chromophores with different excitation spectra can then be selectively addressed by shaping the SH spectrum so as to enhance the target 2PEF signal. To find the optimal spectral phase for a particular application, genetic learning-loop algorithms have often been employed [3,11,12]. Here, with knowledge of the two-photon excitation spectrum of the fluorophore of interest, we simply tune the SH spectrum for selective two-photon fluorescence excitation using a sinusoidal spectral phase [1,2], given by $\varphi(\omega)=A\sin(\gamma(\omega-\omega_0)-\delta)$, where ω_0 is the pulse center frequency and the parameters γ and δ determine the target harmonic frequency. Frequencies ω such that the spectral phase is antisymmetric with respect to $\omega/2$ will yield a vanishing phase factor in Eq. (1), and hence a constructive interference at ω, resulting in an effective excitation of this frequency component identical to that corresponding to a transform-limited pulse – a unique feature of phase shaping as opposed to amplitude shaping. In contrast, the SH spectrum will vanish for other frequency values due to destructive interferences. This process, known as multiphoton intrapulse interference [2], allows selective excitation of the chromophore of interest with a narrowband SH spectrum, the target frequency being controlled through the spectral phase of the shaped pulses.

Compared to the straightforward tuning of a narrowband laser pulse, one of the major advantages of shaping a broadband pulse as described above is the potential for rapid switching between different pulse shapes. However, most experiments to date have been based on liquid-crystal pulse shapers, with switching times limited to tens of milliseconds [7,8]. While various methods have been demonstrated to increase the switching frequency of such pulse shapers [13-15], we chose in this study to use a different technology, based on an acousto-optic programmable dispersive filter known as the Dazzler pulse shaper [16]. This device allows switching between two different pulse shapes at a high rate (10 kHz in our experiment), enabling the quasi-simultaneous acquisition of two images corresponding to pulse shapes chosen to alternately optimize the excitation of eGFP and endogenous fluorescence.

To demonstrate the ability to acquire images associated with selective excitation of the fluorescence, we chose to image live eGFP-labelled *Drosophila* embryos, namely the sGMCA transgenic *Drosophila* line [17], expressing eGFP fused with actin-binding moesin fragments. This line exhibits fluorescence labeling of the cytoskeleton and provides a fluorescent outline of cell shape [17]. Embryos were collected and selected during cellularization (just before gastrulation [18]), dechorionated, and glued to a coverslip [19]. Embryos were mounted in Phosphate Buffered Saline (PBS), covered with a coverslip to produce an observation cell of 300 ± 25 μm thickness, and observed at room temperature. At cellularization, cells (and eGFP fluorescence) are confined to a band just beneath the vitelline membrane that surrounds the

#9986 - $15.00 USD Received 20 December 2005; revised 13 January 2006; accepted 14 January 2006

embryo. The interior of the embryo (yolk) contains no eGFP, but fluoresces due to endogenous species. This strain therefore provided an ideal live system with spatially separated regions of endogenous and eGFP fluorescence that could be readily compared. We first measured the 2PEF yield as a function of excitation wavelength using a femtosecond Titanium:sapphire oscillator (Coherent), delivering 150 fs pulses with a spectral width of 7 nm at a central wavelength of 800 nm, and tunable in the 700-950 nm range. The relative excitation spectrum of eGFP and embryo endogenous fluorescence, shown in Fig. 1(A), was obtained by acquiring images of the whole embryo using a 20x, 0.8 NA objective (Olympus) and dividing the signal measured in the outer region of the embryo (containing eGFP) by the yolk 2PEF signal. These data confirm that, near 820 nm, the excitation spectrum of eGFP increases towards longer wavelengths, while endogenous fluorescence, which arises from fluorophores with emission spectra similar to that of NADH, shows the opposite trend [20-22].

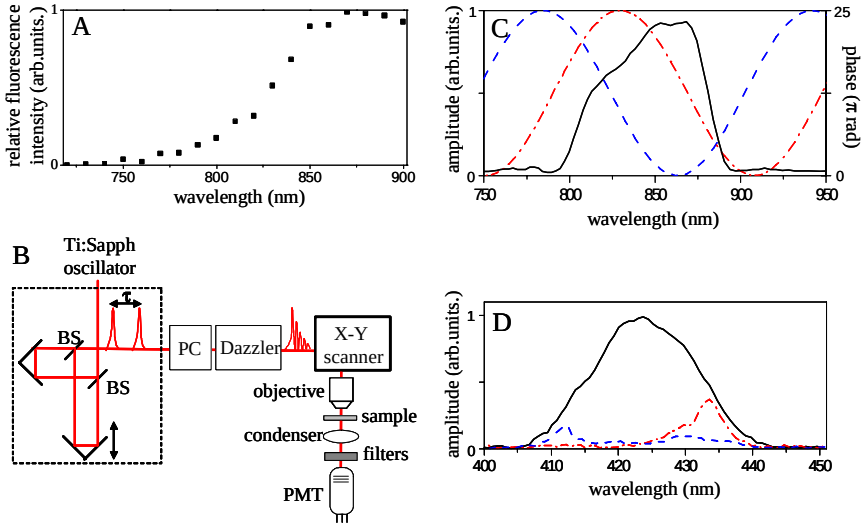

Fig. 1. (a) 2PEF ratio of eGFP/yolk, as measured with a narrow-(b) Experimental setup. BS: beamsplitter, PC: prism compressor, PMT: photomultiplier tube. The interferometer, shown within the dashed box, was used only for characterizing the shaped pulses and was otherwise bypassed. (c) Spectral amplitude (solid line) for the pulses used in the experiments, as well as the applied sinusoidal phase for the red (dash-dot) and blue (dotted) phase-shaped pulses. (d) Corresponding SH spectra for the TL (solid), red-shaped (dash-dot) and blue-shaped (dotted) pulses. The TL amplitude has been reduced by a factor of two for easier comparison with the other spectra. The applied phases for the red and blue-shaped pulses were sinusoidal as defined in the text, with parameters $A = 25\pi$ rad, $\gamma = 0.09$ rad/THz for both pulses. The offset values used for the red and blue-tuned pulses were $\delta = -1.85$ rad and $\delta = -0.1$ rad respectively.

The coherent-control imaging experimental setup is shown in Fig. 1(b). The laser source was a broadband (~20 fs), homebuilt Ti:sapphire oscillator (300 mW, 100 MHz, center wavelength 820 nm). Before reaching the microscope, the laser pulses were phase-shaped using an acousto-optic programmable pulse shaper (Dazzler, Fastlite) [16,23], inserted into the beam path. We precompensated the microscope dispersion with a combination of the Dazzler and a fused-silica prism compressor [24], which we optimized via second-order autocorrelations in a GaAsP two-photon photodiode at the sample position [25]. Imaging was performed using a custom-built scanning microscope incorporating galvanometer mirrors (GSI Lumonics), an Olympus LMPLAN IR 20X, 0.4 numerical aperture objective and a photon-counting photomultiplier tube (PMT) (Electron Tubes PC25) [26]. The excitation power was 12 mW at the sample. The fluorescence signal was detected in the forward direction, after removing through spectral filtering (Chroma E700SP) the transmitted fundamental light.

#9986 - $15.00 USD Received 20 December 2005; revised 13 January 2006; accepted 14 January 2006

Using the Dazzler, we generated two phase-shaped pulses with SH spectra tuned towards respectively low- and high- frequencies, in order to enhance the excitation of respectively the endogenous and eGFP fluorescences. These two pulses, obtained by choosing appropriate values of the δ parameter, will be hereafter referred to as the red-shaped and blue-shaped pulses. Using the interferometer shown in Fig. 1(b), we first characterized the fundamental (Fig. 1(c)) and SH spectra (Fig. 1(d)) of the pulses through linear and nonlinear Fourier-transform spectroscopy as described previously [4]. Figure 1(c) also shows the sinusoidal spectral phase corresponding to the two pulse shapes, which produced the SH spectra shown in Fig. 1(d). We also performed the imaging with transform-limited (TL) pulses (solid line in Fig. 1(d)).

The use of the Dazzler with a 100 MHz femtosecond oscillator requires special care due to the continuous drift between the acoustic waveform propagating in the acousto-optic crystal and the femtosecond pulse train. This drift causes spectral amplitude clipping for pulses that are diffracted when the acoustic waveform is not entirely present inside the crystal. Furthermore, even when the acoustic waveform is entirely inside the crystal, successive femtosecond pulses will be diffracted at different longitudinal positions, and will consequently encounter different amounts of dispersion due to the difference in group velocity dispersion between the ordinary and extraordinary axis. In order to avoid this effect, pulses corresponding to a well-defined position of the acoustic waveform in the crystal must be selected. This can be achieved either at the detection level or at the laser level using a modulator. For simplicity, the former method was implemented here by gating the fluorescence photon counts using a TTL signal synchronized with respect to the Dazzler waveform trigger. With the femtosecond oscillator as a 100-MHz clock, it was possible to select the start and stop position of the gating signal using home-made electronics based on a Complex Programmable Logic Device (M4A3-128/64-55, Lattice Semiconductor Corporation). In order to ensure a good compromise between a large fluorescence signal and a homogenous distribution of pulse shapes, we used a gating width corresponding to 300 oscillator pulses, *i.e.* 6% of the total number of pulses delivered by the oscillator for each acoustic waveform. Note that a similar gating procedure was used for recording the data shown in Fig. 1(C) and 1(D) so that the characterized spectra correspond to those actually used in the imaging experiment.

Figure 2 shows fluorescence images of a live eGFP labeled *Drosophila* embryo recorded with different phase-shaped pulses, where Fig. 2(a) and 2(b) are the images obtained quasi-simultaneously using blue- and red-shaped pulses respectively. A perfect synchronization at the pixel level was obtained between these two images by alternating the acoustic waveform sent into the Dazzler at 10 kHz. Figure 2(c) shows the image obtained using transform limited pulses which excite the membrane-labelled eGFP, as well as significant endogenous fluorescence in the yolk and vitelline membrane. This should be compared with the blue-shaped pulse, which produces higher fluorescence from the yolk (Fig. 2(a)). Conversely, the red-shaped pulse shows significantly reduced yolk fluorescence and enhanced fluorescence from the eGFP-labelled cytoskeleton (Fig. 2(b)). This difference is readily apparent in Fig. 3, which displays the fluorescence profile along a line (position shown in Fig. 2(c)) through the embryo. The efficiency of the chromophore selection can be described by the contrast factor

$$\Gamma = \frac{R_{blue} - R_{red}}{R_{blue} + R_{red}} \tag{2}$$

where R_{blue} and R_{red} are ratios of emission between the yolk and eGFP regions for blue-shaped and red-shaped pulses respectively. From the graph shown in Fig. 3, we obtain a contrast $\Gamma = 0.35$, in good agreement with the expected value $\Gamma = 0.39$ obtained from the

#9986 - $15.00 USD Received 20 December 2005; revised 13 January 2006; accepted 14 January 2006

excitation spectrum shown in Fig. 1(a), assuming switching between 412 and 435-nm SH excitation wavelengths.

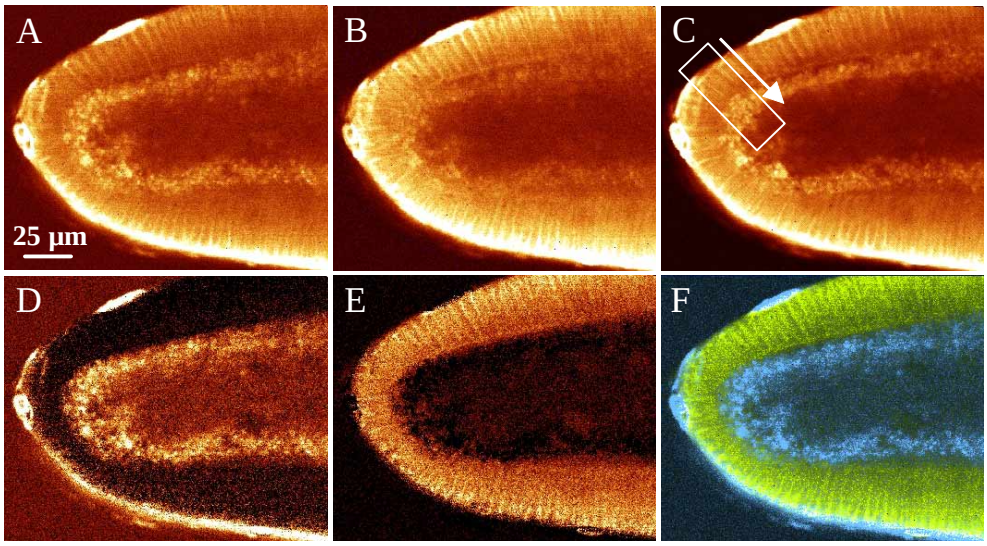

Fig. 2. 2PEF images of an eGFP labeled *Drosophila* embryo. (a) Blue-tuned excitation. (b) Red-tuned excitation. (c) Transform limited pulse. These three images are normalized to the fluorescence signal of the vitelline membrane. (d) Linear combination of A and B to isolate the eGFP fluorescence. (e) Linear combination of A and B to isolate the yolk fluorescence. (f) Composite image of C and D to illustrate the good separation between eGFP and yolk fluorescence.

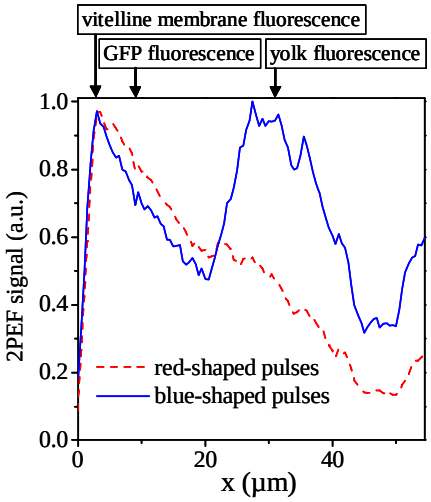

Fig. 3. 2PEF signal profiles for the shaped pulses through the section indicated in Fig. 2(C), showing significantly different signal levels in the eGFP and yolk.

As a side-effect of enhanced selectivity, we observe that the fluorescence yield in the case of the shaped pulses is about 8 to 17% of that for a TL pulse, due to the smaller overlap between the SH spectra shown in Fig. 1(d) and the chromophore absorption spectra. However we note that amplitude shaping resulting in the same SH spectral width would have resulted in a much greater reduction in two-photon excitation efficiency because fewer spectral components would then contribute to chromophore excitation. In general, an appropriate choice for the

#9986 - $15.00 USD Received 20 December 2005; revised 13 January 2006; accepted 14 January 2006

spectral phase results from a compromise between optimizing the contrast factor Γ and matching the spectral width of the SH spectrum with that of the chromophore absorption spectrum.

A unique feature of a quasi-simultaneous acquisition of images associated with two different pulse shapes is that it enables the computation of linear combinations of the two images, owing to the perfect correspondence between pixels of identical coordinates. Such a procedure permits the removal of the inevitable crosstalk ($\Gamma < 1$) resulting from the overlap between the excitation spectra of the imaged species. This method is demonstrated in Fig. 2(d) and 2(e), which are linear combinations of the quasi-simultaneously acquired blue and red-shaped images shown in Fig. 2(a) and (b). The coefficients used in the linear combination were determined by selecting two areas of the embryo image in the yolk and in the cell layer region and assuming that the 2PEF signal originated from the endogenous and eGFP fluorescence respectively. Fig. 2(f) is a superposition of the images in Fig. 2(D) and (E), coloured to indicate the respective contributions. This picture clearly illustrates the ability to distinguish eGFP from endogenous fluorescence contributions using phase-shaped laser pulses.

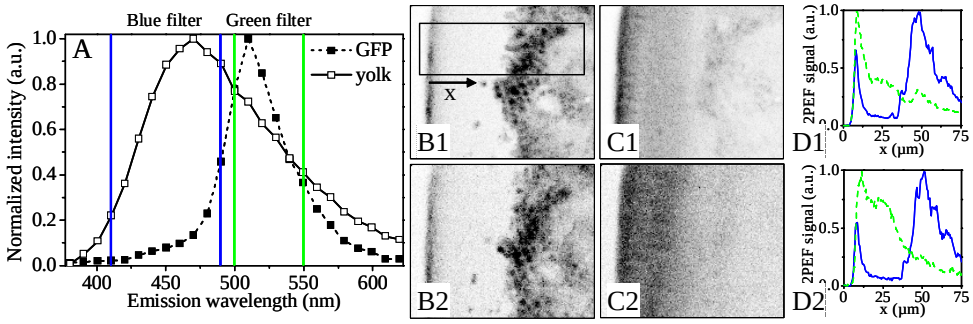

Fig. 4. A) 2PEF spectra of yolk and eGFP measured in vivo under 820-nm excitation by recording the descanned epidetected fluorescence filtered using a 15-nm tunable interferential filter (S-60, Schott) . Also shown are the wavelength ranges selected by the emission filters. B1) 2PEF images using blue-filter for TL and B2) blue-shaped pulses. C1) 2PEF images using green-filter for TL and C2) red-shaped (right) pulses. D1) X-profile for TL and D2) shaped pulses with filters at location indicated in B1.

A common approach to separating several types of fluorophores is to spectrally filter their fluorescence emissions. This becomes difficult if there is considerable overlap in the emission spectra, and is accompanied by significant loss of fluorescence signal and poor selectivity. In the case of eGFP and yolk fluorescence, the spectral overlap is large, as shown in Fig. 4(a). We therefore explored how the combined use of shaped pulses and filters could enhance the selectivity achievable with spectral filters alone. Figures 4(b1) and 4(b2) show images that have been spectrally filtered with the blue filter indicated in Fig. 4(a). Figure 4(b1) used TL excitation, while Fig. 4(b2) was taken with the blue-shaped pulses. Similarly, images that were recorded with the green filter are shown in Fig. 4(c1) and Fig. 4(c2), where TL excitation and red-shaped pulses were used respectively. Figures 4(d1) and 4(d2) show the profile, along the box indicated in Fig. 4(b), for the TL and shaped excitation respectively, allowing a comparison of the selectivity provided by using emission filters alone, or a combination of emission filters and phase-shaping. In the filters-only case, the blue filter is quite effective at removing the eGFP fluorescence. However, the green filter does not completely select the eGFP signal, leaving a significant amount of yolk fluorescence. When the filters are combined with phase-shaping, the images show a significant enhancement of the contrasts obtained with the two spectral filters by nearly a factor of 3. This enhancement demonstrates that a combination of phase-shaping and spectral filtering results in better selectivity than spectral filtering alone. This will be true in all cases where emission spectra overlap significantly but excitation spectra are more distinct, and provides an additional

#9986 - $15.00 USD Received 20 December 2005; revised 13 January 2006; accepted 14 January 2006

degree of freedom beyond emission filtering for achieving selectivity. As an illustrating example, distinguishing between CFP (Cyan Fluorescent Protein) and NADH through spectral filtering of the 2PEF signal would be particularly difficult due to their very similar emission spectra [20,22]. However, the excitation spectra of these two species present significant differences [22,27], which suggests that pulse shaping would be an efficient tool for their selective imaging.

Phase-only shaping may also have advantages for multiplex fluorescence imaging of fluorophores with significantly different 2PEF cross-sections. In this case, optimizing the excitation conditions can be challenging because different exposure times are necessary to achieve comparable image quality for the different fluorophores. This often requires sacrificing excess signal from the higher cross-section emitter. Phase-shaping can address this problem by choosing the appropriate relative number of red or blue shaped pulses to balance the emission levels, thus more efficiently using the excitation light and avoiding unnecessary illumination of the sample that could lead to photodamage.

The use of a programmable, rapid pulse-shaper allows flexibility in determining optimum phase-shaping for specific imaging conditions. However, once the optimum spectral phase has been determined, the pulse-shaper could easily be replaced by a static phase-mask that provides the required spectral phase shape. This method would have the benefit of using all the oscillator pulses, resulting in shorter acquisition times than the 7 mn required for each of the images shown in Fig. 2(a) and 2(b). Such an approach would be directly analogous and complementary to spectral filtering of the emission. Rapid switching between different static phase masks for multiplex imaging could be achieved by a scanning mirror [14] or an acousto-optic beam deflector. Our current implementation permits selective excitation over the bandwidth of the laser source (~100 nm) with a single laser source. Extending this range is desirable to access a broader range of fluorophores, and may be possible through phase-shaping of continua generated by a photonic crystal fiber [28]. This would remove the need for multiple laser sources while providing access to a wide range of fluorophores that could be rapidly and selectively excited. This possibility is particularly attractive for ratiometric imaging [29]. A broader spectral range will also be of great practical interest for the important application of imaging transgenic animals. Fast shaping approaches will allow simultaneous addressing of a collection of fluorophores such as fluorescent proteins-based constructs (CFP, YFP, cameleons, etc.) as well as endogenous species such as NADH.

In conclusion we have demonstrated the use of spectral phase-shaping for selective two-photon fluorescence imaging of live eGFP labeled *Drosophila* embryos. Employing a fast switching pulse-shaper, we obtained quasi-simultaneous images corresponding to pulse shapes optimized to selectively excite eGFP or endogenous fluorescence. Linear combinations of these images demonstrated that a high degree of selectivity is attainable through phase-shaping. When used in combination with spectral filtering of the emission, we found that phase-shaping improved selectivity between eGFP and endogenous fluorescence by a factor of ~3. Phase-shaping provides an additional dimension towards improving the selectivity and extending the multiplex capabilities of fluorescence microscopy.

Acknowledgments

We thank Emmanuel Farge and Willy Supatto for providing us with the transgenic eGFP labeled *Drosophila* strain and for many discussions. We also thank Kevin Kubarych, Richard Herzog and Thomas Oksenhendler for numerous discussions of the operation of the Dazzler pulse-shaper, as well as Antigoni Alexandrou and Adeline Bonvalet for useful discussions about the experiment. This work was supported by the Délégation Générale pour l'Armement.

#9986 - $15.00 USD Received 20 December 2005; revised 13 January 2006; accepted 14 January 2006